RSC Advances

PAPER

View Article Online
View Journal | View Issue

Cite this: *RSC Adv.*, 2020, **10**, 37369

A study on the self-assembly mode and supramolecular framework of complexes of cucurbit[6]urils and 1-(4-methoxyphenyl) piperazine†

Yanmei Jin, Tinghuan Huang, Weiwei Zhao, Xinan Yang, Ye Meng and Peihua Ma *

Received 18th September 2020
Accepted 29th September 2020

DOI: 10.1039/d0ra07988j

rsc.li/rsc-advances

Self-assembly between symmetrical dicyclohexyl-substituted cucurbit[6]uril (abbreviated as **(CyH)$_2$Q[6]**) and cyclopentanocucurbit[6]uril (**CyP$_6$Q[6]**) as hosts and 1-(4-methoxyphenyl)piperazine (**MeOPP**) as a guest molecule has been studied by means of single-crystal X-ray diffraction analysis, NMR, MALDI-TOF mass spectrometry, and other characterization methods. The experimental results showed that the self-assembly was driven by the formation of exclusion complexes by the cucurbit[*n*]uril and the guest, that is, supramolecular interaction between the negative charge of the cucurbit[*n*]uril portals and a coordination polymer guest. Complexes were formed between the positive charge of the cucurbit[*n*]uril outer wall and inorganic anions, thus generating self-assemblies with multi-dimensional and multi-level supramolecular frameworks.

1. Introduction

Porous materials, such as inorganic zeolites,[1] metal–organic frameworks (MOFs),[2,3] and covalent organic frameworks (COFs),[4,5] have been widely used in heterogeneous catalysis, adsorption, and ion-exchange processes, *etc.*[6–9] In this context, cucurbit[*n*]urils[10–16] are expected to become basic construction units. According to studies of the electrical properties of the surface structure of cucurbit[*n*]urils, the following statements can be made[17] (Scheme 1). (1) The regions around the carbonyl units of the portals bear a significant negative potential, which makes cucurbit[*n*]urils organic ligand molecules with multiple binding sites. Cucurbit[*n*]urils with different degrees of polymerization have portals of different sizes, which can provide coordination environments with different structural characteristics, giving rise to diverse complexes and supramolecular assemblies. This constitutes the coordination chemistry of cucurbit[*n*]urils.[18–21] (2) The inner cavities of cucurbit[*n*]urils are electrically neutral. Cucurbit[*n*]urils with different degrees of polymerization also have cavities of different sizes, which can accommodate guest molecules of different sizes. This constitutes the host–guest chemistry of cucurbit[*n*]urils.[22–24] (3) The outer surfaces of the cucurbit[*n*]urils bear positive electrostatic potentials. This has given rise a new research field[25,26] based on interactions between the outer surface of Q[*n*]s (OSIQ) and electronegative species.

For the present study, we selected 1-(4-methoxyphenyl) piperazine (**MeOPP**), an antihypertensive intermediate of phenylpiperazine, as the guest. As hosts, we selected cucurbit[*n*]urils substituted with cyclopentyl[27] or cyclohexyl groups,[28]

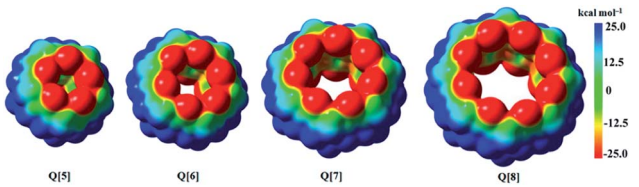

Scheme 1 Electrostatic potential maps (ESPs) for Q[5], Q[6], Q[7], and Q[8], respectively. ESPs are mapped on electron density isosurfaces (0.001 e au^{-3}) for cucurbit[*n*]urils at the B3LYP/6-311G (d, p) level of theory with Gaussian09.

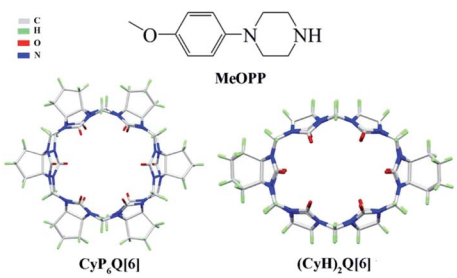

Scheme 2 CyP$_6$Q[6], (CyH)$_2$Q[6], and the guest molecule used in this study.

Key Laboratory of Macrocyclic and Supramolecular Chemistry of Guizhou Province, Guizhou University, Guiyang 550025, People's Republic of China. E-mail: phma@gzu.edu.cn

† Electronic supplementary information (ESI) available. See DOI: 10.1039/d0ra07988j

because these modified cucurbit[*n*]urils (Scheme 2) have better water solubility than unsubstituted cucurbit[*n*]urils.

Single crystal X-ray diffraction analysis, nuclear magnetic resonance (NMR), matrix-assisted laser desorption ionization time-of-flight mass spectrometry (MALDI-TOF), and other characterization methods have been used to study supramolecular self-assembly between the guest molecule and the two cucurbit[*n*]uril hosts. The results showed that the guest and the respective cucurbit[*n*]uril hosts self-assembled through the formation of exclusion complexes, specifically supramolecular interaction between the negative charge of the cucurbit[*n*]uril portal and a coordination polymer guest. Moreover, complexes formed between the positive charge of the outer wall of cucurbit[*n*]uril and the inorganic anions generated self-assemblies with multi-dimensional and multi-level supramolecular frameworks.

2. Experimental

2.1. Experimental equipment and reagents

Symmetrical dicyclohexyl-substituted cucurbit[6]uril (**(CyH)$_2$Q[6]**)[28] and cyclopentanocucurbit[6]uril (**(CyP)$_6$Q[6]**)[27] were prepared and purified in accordance to a literature method. All reagents were obtained in analytically pure form. Diffraction data for the complexes were collected at 273.15 K on a Bruker D8 VENTURE diffractometer or a Bruker SMART Apex-II CCD diffractometer. NMR spectra were recorded on a Varian INOVA 400M spectrometer. MALDI-TOF mass spectrometry was performed on an Agilent 6545 Q-TOF mass spectrometer.

2.2. Synthesis of the complexes

The **(CyH)$_2$Q[6]** (15 mg, 14.6 mmol) was placed in a beaker and taken up in 6 M hydrochloric acid (10 mL). **MeOPP** (15.4 mmol) was taken up in distilled water (3 mL), which was heated to aid dissolution. The latter solution was then poured into the former. Finally, a small amount of the inducing agent $CdCl_2$ was added, and the solution was heated and stirred for 10 min in a water bath at 30 °C, cooled to room temperature, and allowed to stand. After 3 weeks, colorless single crystals suitable for crystal structure determination had precipitated (43% yield). Complex **2** was synthesized in a similar manner as complex **1** in a yield of 39%.

2.3. Crystal measurement

A measurable (transparent and crack-free) crystal of the complex of appropriate size was selected, fixed on a glass fiber with vaseline, and introduced into the Bruker Smart Apex II single-crystal X-ray diffractometer to collect diffraction data. An Mo target was adopted; excitation voltage 20 kV; wavelength (λ(Mo-K$_\alpha$)) 0.71073 Å. The SHELXT-14 program was used for structure analysis, and the SHELXL-14 program was used for data refinement by a full-matrix least-squares method. The SQUEEZE routine of PLATON was used to remove some solvent molecules from the crystal. CCDC-2021200 (**1**) and CCDC-2021162 (**2**) contain the crystal data for this paper. The main crystal structure parameters are shown in Table 1.

Table 1 Crystallographic data for the complexes

	1	**2**
Empirical formula	$C_{55}H_{64}N_{26}O_{13}$	$C_{65}H_{76}N_{26}O_{13}$
Formula weight	1297.286	1429.492
Crystal system	Triclinic	Monoclinic
Space group	$P\bar{1}$	$C12/c1$
a [Å]	14.944(3)	29.984(8)
b [Å]	15.743(4)	13.001(2)
c [Å]	19.200(4)	25.823(7)
α [°]	90.039(8)	90
β [°]	90.099(8)	111.150(14)
γ [°]	112.980(8)	90
V [Å^3]	4158.6(15)	9388(4)
Z	1	1
D_{calcd} [g cm^{-3}]	2.820	0.034
T [K]	273.15	273.15
μ [mm^{-1}]	5.269	0.063
Parameters	1065	622
R_{int}	0.0552	0.0699
R [$I > 2\sigma(I)$][a]	0.0538	0.0461
wR [$I > 2\sigma(I)$][b]	0.1498	0.1112
R (all data)	0.0775	0.0755
wR (all data)	0.1686	0.1291
GOF on F^2	1.028	1.040

[a] Conventional R on F_{hkl}: $\sum||F_o| - |F_c||/\sum|F_o|$. [b] Weighted R on $|F_{hkl}|^2$: $\sum[w(F_o^2 - F_c^2)^2]/\sum[w(F_o^2)^2]^{1/2}$.

2.4. Determination by ^{1}H NMR

A 2.0–2.5 × 10^{-3} mmol L^{-1} solution of the guest was prepared in D_2O. It was then added dropwise to a solution of the cucurbituril (0.5–0.7 g) in D_2O. The spectral changes were monitored on a Varian Inova 400M NMR spectrometer at 20 °C.

2.5. Determination by mass spectrometry

The sample was prepared as a 10 μg mL^{-1} solution in doubly-distilled water, which was filtered into a chromatographic sample bottle through an aqueous 0.22 μm filter membrane. Mass spectra were recorded on an Agilent 6545 Q-TOF mass spectrometer.

3. Results and discussion

3.1. Description of the crystal structures of complexes 1 and 2

3.1.1. Description of the crystal structure of complex 1. Fig. 1(f) shows the supramolecular self-assembly formed from **(CyH)$_2$Q[6]**, **MeOPP**, and $[CdCl_4]^{2-}$. In this self-assembly, the carbonyl oxygen atoms at the **(CyH)$_2$Q[6]** portal interacted with the **MeOPP** molecule through hydrogen-bonding and ion–dipole interactions. Specifically, the proton (H26A) on the nitrogen of the **MeOPP** molecule interacted with the carbonyl oxygen atoms (O3, O4) at the **(CyH)$_2$Q[6]** portal through ion–dipole interactions. The carbonyl oxygen atoms (C=O) at the portal of **(CyH)$_2$Q[6]** were connected with the heterocycle of the **MeOPP** molecule through hydrogen-bonding with distances in the range 2.165–2.687 Å. There was a weak π···π interaction between the carbonyl oxygen atom of the **(CyH)$_2$Q[6]** portal and the benzene ring of **MeOPP** (2.333 Å) [Fig. 1(a)]. Two adjacent

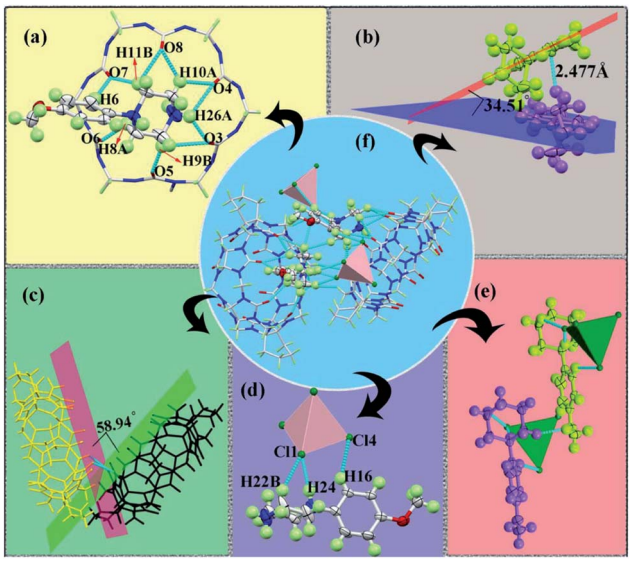

Fig. 1 (a) Crystal diagram of complex **1**; (b) the interaction of adjacent guest molecules; (c) the interaction of adjacent **(CyH)$_2$Q[6]** molecules; (d and e) the interaction of **MeOPP** molecules with $[CdCl_4]^{2-}$; (f) supramolecular self-assembly of complex **1**.

MeOPP molecules formed an angle of 34.51° with the plane of the benzene ring, and were connected by a hydrogen-bonding dislocation interaction (2.477 Å) [Fig. 1(b)]. Two adjacent **(CyH)$_2$Q[6]** molecules formed an angle of 58.94° with the plane of the terminal carbonyl group, which were connected by a dipole–dipole dislocation interaction [Fig. 1(c)]. The $[CdCl_4]^{2-}$ anion interacted with the **MeOPP** molecule through ion–dipole interactions [Fig. 1(d and e)].

Fig. 2(b) shows the stacking diagram of complex **1**. The supramolecular framework of **(CyH)$_2$Q[6]@MeOPP** was formed by dipole–dipole interactions between molecules of **(CyH)$_2$Q[6]** and weak interactions between the cucurbituril and the guest, assisted by surrounding $[CdCl_4]^{2-}$ anions. In the *c*-direction, the adjacent cucurbituril molecules were arranged in a V-shape with **MeOPP** molecules through OSIQ induced by the anions [Fig. 2(a)]. Two-dimensional surfaces were formed between layers through self-induction and anion induction [Fig. 1(c)], whereby **MeOPP** molecules were connected by hydrogen bonds and coordinate with surrounding $[CdCl_4]^{2-}$ anions through weak interactions [Fig. 2(d)]. A cucurbituril molecule interacted with four $[CdCl_4]^{2-}$ anions through anion-induced OSIQ [Fig. 2(e)], while the cucurbituril portal and outer wall were connected to six guest molecules through weak interaction, among which four guest molecules interacted with the cucurbituril portals and the other two guest molecules were connected to methylene ($-CH_2$) units on outer wall of the cucurbituril molecule through hydrogen-bonding [Fig. 2(f)].

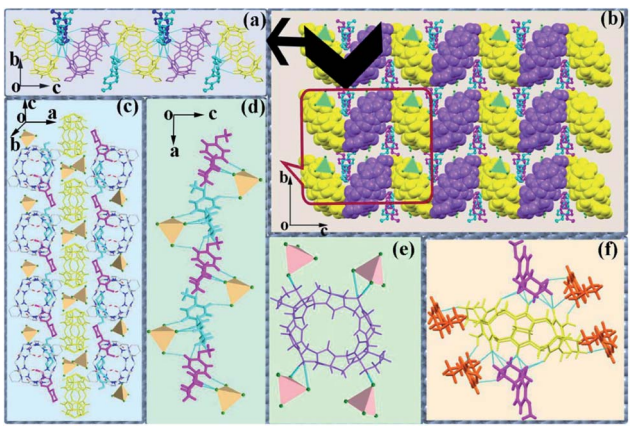

Fig. 2 Crystal structure of complex **1**: (a) 1D chain structure of the assembly **1**. Hydrogen atoms are omitted for clarity. (b) Overview of supramolecular assembly in complex **1**; (c) interaction between layers; (d) interaction between moieties; (e) Representative anion-induced OSIQ between a **(CyH)$_2$Q[6]** molecule and neighbouring anions. Interaction between **(CyH)$_2$Q[6]** and neighboring $[CdCl_4]^{2-}$ anions; (f) interaction between **(CyH)$_2$Q[6]** and the surrounding **MeOPP** molecules.

3.1.2. Description of the crystal structure of complex 2. Fig. 3(b) shows the supramolecular self-assembly formed by **CyP$_6$Q[6]**, **MeOPP**, and $[CdCl_4]^{2-}$. In this self-assembly, the interaction mode of the guest molecule was similar to that in complex **1**. The protons (H1, H2A, H2B) on the N atoms of the **MeOPP** molecule and the carbonyl oxygen atoms (O4, O10, O11) at the cucurbituril portal were engaged in ion–dipole interactions (1.962–2.552 Å). The carbonyl oxygen atoms (C=O) at the portal of **CyP$_6$Q[6]** were connected with the heterocycle of **MeOPP** by hydrogen-bonding, with distances in the range 2.164–2.522 Å. There was also a weak π···π interaction (2.632 Å) between a carbonyl oxygen atom at the portal of **CyP$_6$Q[6]** and the benzene ring of **MeOPP** [Fig. 3(a and c)].

It can be observed from Fig. 4(a) that one cucurbituril molecule interacted with six $[CdCl_4]^{2-}$ anions through anion-induced OSIQ. This was different from the situation in complex **1** in that $[CdCl_4]^{2-}$ anions were engaged in ion–dipole interactions with bridging "waist" methylene ($-CH_2$) units of **CyP$_6$Q[6]**. A **CyP$_6$Q[6]** molecule was surrounded by four **MeOPP** molecules through noncovalent bonds, whereby two guest molecules interacted with the cucurbituril portal through weak interactions, and the other two guest molecules interacted with the "waist" methylene ($-CH_2$) units of the bridging **CyP$_6$Q[6]** molecule through hydrogen bonds [Fig. 4(b)]. There was hydrogen-bonding between the carbonyl oxygen atoms at the portal of one cucurbituril molecule and the methylene ($-CH_2$) units of another adjacent cucurbituril [Fig. 4(c)]. Fig. 4(d) shows the general situation of supramolecular assembly in complex **2**, in which $[CdCl_4]^{2-}$ anions surrounded each **CyP$_6$Q[6]** molecule

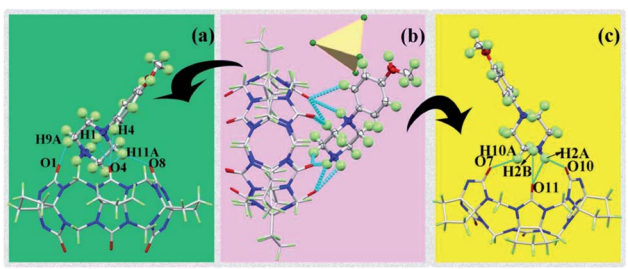

Fig. 3 Crystal diagram of complex **2**: (a and c) interactions between **CyP$_6$Q[6]** and **MeOPP**; (b) supramolecular self-assembly of complex **2**.

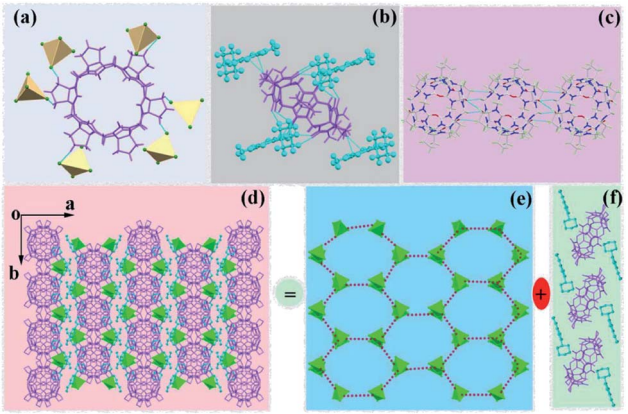

Fig. 4 Crystal structure of complex **2**: (a) representative anion-induced OSIQ between a $CyP_6Q[6]$ molecule and neighboring anions; (b) interactions between $CyP_6Q[6]$ and surrounding **MeOPP** molecules; (c) interaction between melon rings; (d) overview of supramolecular assembly in complex **2**; (e) $[CdCl_4]^{2-}$ hexagonal honeycomb framework; (f) 1D chain structure of the assembly **2**. Hydrogen atoms are omitted for clarity.

to form a hexagonal honeycomb framework [Fig. 4(e)]. Each unit in the framework was filled with coordination polymer based on **$CyP_6Q[6]$@MeOPP** [Fig. 4(f)], and the cucurbituril was surrounded by guest molecules through weak interactions, thus forming a two-dimensional surface. Salient bond lengths in the complexes are shown in Table 2.

3.2. ^{1}H NMR and MALDI-TOF mass spectrometric analysis of cucurbiturils and guests

3.2.1. ^{1}H NMR spectra of cucurbiturils and guests. NMR is one of the most commonly used and effective methods for studying host–guest chemistry. When the molar ratio of the guest to the host was 0.25 (Table 3), all of the proton signals of the guest shifted to lower field, indicating that the whole guest molecule was located within the portals of the respective cucurbiturils, and was thus de-shielded by the cucurbituril. Meanwhile, the chemical shifts of protons far away from the piperazine moiety showed little change.

Table 2 Partial bond length data for complexes **1** and **2**

Complexes	Bond	Bond length/Å
1	H9B–O3	2.165
	H9B–O5	2.687
	H8A–O6	2.382
	H6–O7	2.333
	H11B–O8	2.681
	H10A–O8	2.519
	H10A–O4	2.454
	H26A–O4	2.277
	H26A–O3	2.180
	H38A–O3	2.556
	H60A–O12	2.656
	Cl1–H22B	2.828
	Cl1–H24	2.149
	Cl4–H16	2.834
2	H1–O4	2.536
	H2A–O11	2.363
	H2B–O11	2.552
	H2A–O11	1.962
	H10A–O7	2.368
	H9A–O1	2.503
	H11A–O4	2.522
	H11A–O8	2.164
	H4–O4	2.632

Table 3 ^{1}H NMR data of interaction between cucurbiturils and guest

Complex	H_α	H_β	H_γ	H_δ	H_ε
MeOPP	7.01	6.91	3.67	3.28	3.25
n(**MeOPP**)/n(**$(CyH)_2Q[6]$**) = 0.25	−0.40	−0.06	−0.12	−0.42	−0.39
n(**MeOPP**)/n(**$CyP_6Q[6]$**) = 0.25	−0.21	−0.01	−0.02	−0.28	−0.24

Fig. 5 shows ^{1}H NMR titration spectra obtained upon adding free guest to the cucurbiturils. In Fig. 5(A), (a) is the NMR spectrum of **$(CyH)_2Q[6]$**, (b–d) are the NMR spectra when n(**MeOPP**)/n(**$(CyH)_2Q[6]$**) is equal to 0.25, 0.75, and 1, and (e) is the NMR spectrum of the free guest. As the concentration of the guest was increased, the proton signals shifted towards lower field to varying degrees, indicating that **MeOPP** molecules interact with the outer walls of the cucurbiturils. This is consistent with the single-crystal X-ray diffraction characterization. The ^{1}H NMR titration spectra of **$CyP_6Q[6]$@MeOPP** are similar to those of **$(CyH)_2Q[6]$@MeOPP**, and so are not described in detail.

3.2.2. Mass spectrometry. In order to further understand the interaction mode of the host and guest, we used matrix-assisted laser desorption/ionization time-of-flight mass spectrometry to characterize the structures of the complexes, as shown in Fig. 6. The **$(CyH)_2Q[6]$@MeOPP** and **$CyP_6Q[6]$@MeOPP** systems showed obvious molecular ion peaks at m/z 1297.5177 and 1429.6175, respectively. These molecular ion peaks could be attributed to [**$(CyH)_2Q[6]$** + **MeOPP** + H]$^+$ and [**$CyP_6Q[6]$** + **MeOPP** + H]$^+$ (theoretical calculated m/z values 1297.549 and 1429.6158, respectively). The results show that the host and guest interact in a 1 : 1 ratio, consistent with the results of the above analysis.

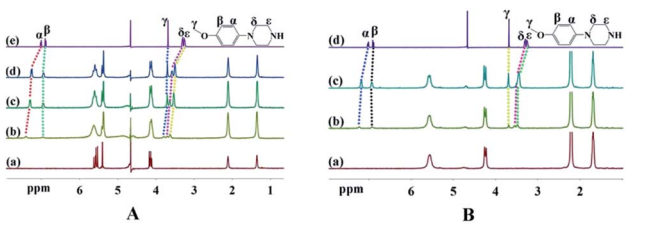

Fig. 5 (A) $(CyH)_2Q[6]$@MeOPP ^{1}H NMR titration spectra: (a) ^{1}H NMR spectrum of $(CyH)_2Q[6]$; (b) n(MeOPP)/n($(CyH)_2Q[6]$) = 0.25; (c) n(MeOPP)/n($(CyH)_2Q[6]$) = 0.75; (d) n(MeOPP)/n($(CyH)_2Q[6]$) = 1; (e) free guest MeOPP; (B) ^{1}H NMR titration spectra of $CyP_6Q[6]$@MeOPP: (a) ^{1}H NMR spectrum of $CyP_6Q[6]$; (b) n(MeOPP)/n($CyP_6Q[6]$) = 0.25; (c) n(MeOPP)/n($CyP_6Q[6]$) = 1; (d) free guest MeOPP.

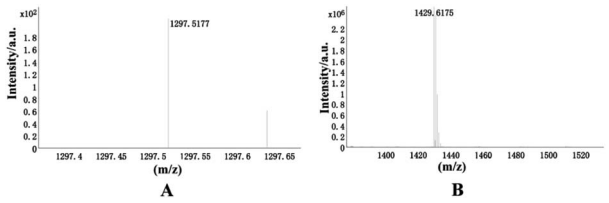

Fig. 6 MALDI-TOF mass spectra of $(CyH)_2Q[6]$@MeOPP and $CyP_6Q[6]$@MeOPP.

4. Conclusions

In this article, it shows that 1-(4-methoxyphenyl)piperazine (**MeOPP**) interacted with symmetrical dicyclohexyl-substituted cucurbit[6]uril (**$(CyH)_2Q[6]$**) and cyclopentanocucurbit[6]uril (**$CyP_6Q[6]$**) under hydrothermal conditions in the presence of $CdCl_2$ as an inducer to construct two different supramolecular self-assemblies. These two self-assembled structures have been characterized by single crystal XRD analysis, NMR, and MALDI-TOF mass spectrometry.

Our experiments have shown that, in the presence of $CdCl_2$ as an inducer, the heterocycle of the **MeOPP** molecule acted like a "lid" connected to the carbonyl oxygen atoms of the cucurbituril portals. Moreover, the benzene ring and cucurbituril were also engaged in a weak $\pi\cdots\pi$ interaction, thereby making the guest molecule more firmly bound at the cucurbituril portal. The outer wall of melon rings interacted with multiple $[CdCl_4]^{2-}$ anions through anion-induced OSIQ, and the rings were connected by hydrogen bonds to form a two-dimensional supramolecular self-assembly.

A difference was that there was a dislocation arrangement between adjacent cucurbituril moieties in complex **1**, and there was also a dislocation arrangement between the guests; on the contrary, there was a parallel arrangement in complex **2**.

Conflicts of interest

There are no conflicts to declare.

Acknowledgements

This work was financially supported by the National Natural Science Foundation of China (Grant No. 21762011) and Guizhou Science and Technology Planning Project (Guizhou Science and Technology Cooperation Platform Talent [2017]5788).

Notes and references

1 M. Dusselier and M. E. Davis, *Chem. Rev.*, 2018, **118**, 5265–5329.
2 O. M. Yaghi, G. M. Li and H. L. Li, *Nature*, 1995, **378**, 703–706.
3 A. Helal, Z. H. Yamani, K. E. Cordova and O. M. Yaghi, *Natl. Sci. Rev.*, 2017, **4**, 296–298.
4 H. Wang, Z. T. Zeng, P. Xu, L. S. Li, G. G. Zeng, R. Xiao, Z. Y. Tang, D. L. Huang, L. Tang, C. Lai, D. N. Jiang, Y. Liu, H. Yi, L. Qin, S. J. Ye, X. Y. Ren and W. W. Tang, *Chem. Soc. Rev.*, 2019, **48**, 488–516.
5 P. J. Waller, F. Gandara and O. M. Yaghi, *Acc. Chem. Res.*, 2015, **48**, 3053–3063.
6 Y. H. Wen, J. Zhang, Q. Xu, X. T. Wu and Q. L. Zhu, *Coord. Chem. Rev.*, 2018, **376**, 248–276.
7 J. Y. Kim, H. Oh and H. R. Moon, *Adv. Mater.*, 2019, **31**, 1805293.
8 S. S. Han, J. L. Mendoza-Cortes and W. A. Goddard III, *Chem. Soc. Rev.*, 2009, **38**, 1460–1476.
9 G. Chedid and A. Yassin, *Nanomaterials*, 2018, **8**(11), 916.
10 D. Whang, J. Heo, J. H. Park and K. Kim, *Angew. Chem., Int. Ed.*, 1998, **37**, 78–80.
11 L. Isaacs, *Chem. Commun.*, 2009, 619–629.
12 A. I. Day, R. J. Blanch, A. P. Arnold, S. Lorenzo, G. R. Lewis and I. Dance, *Angew. Chem., Int. Ed.*, 2002, **41**, 275–277.
13 L. Isaacs, S. K. Park, S. M. Liu, Y. H. Ko, N. Selvapalam, Y. Kim, H. Kim, P. Y. Zavalij, G. H. Kim, H. S. Lee and K. Kim, *J. Am. Chem. Soc.*, 2005, **127**, 18000–18001.
14 X. Xiao, J. X. Liu, Z. F. Fan, K. Chen, Q. J. Zhu, S. F. Xue and Z. Tao, *Chem. Commun.*, 2010, **46**, 3741–3743.
15 J. Kim, I. S. Jung, S. Y. Kim, E. Lee, J. K. Kang, S. Sakamoto, K. Yamaguchi and K. Kim, *J. Am. Chem. Soc.*, 2000, **122**, 540–541.
16 S. M. Liu, K. Kim and L. Isaacs, *J. Org. Chem.*, 2007, **72**, 6840–6847.
17 X. L. Ni, X. Xiao, H. Cong, Q. J. Zhu, S. F. Xue and Z. Tao, *Acc. Chem. Res.*, 2014, **47**, 1386–1395.
18 M. N. Sokolov, M. N. Dybtsev and V. P. Fedin, *Russ. Chem. Bull.*, 2003, **52**, 1041–1060.
19 O. A. Gerasko, M. N. Sokolov and V. P. Fedin, *Pure Appl. Chem.*, 2004, **76**, 1633–1646.
20 V. P. Fedin, *Russ. J. Coord. Chem.*, 2004, **30**, 151–158.
21 X. L. Ni, X. Xiao, H. Cong, L. L. Liang, K. Chen, X. J. Cheng, N. N. Ji, Q. J. Zhu, S. F. Xue and Z. Tao, *Chem. Soc. Rev.*, 2013, **42**, 9480–9508.
22 K. Kim, *Chem. Soc. Rev.*, 2002, **31**, 96–107.
23 J. Lagona, P. Mukhopadhyay, S. Chakrabarti and L. Isaacs, *Angew. Chem., Int. Ed.*, 2005, **44**, 4844–4870.
24 E. Masson, X. Ling, R. Joseph, L. Kyeremeh-Mensah and X. Lu, *RSC Adv.*, 2012, **2**, 1213–1247.
25 F. Zhang, T. Yajima, Y. Z. Li, G. Z. Xu, H. L. Chen, Q. T. Liu and O. Yamauchi, *Angew. Chem., Int. Ed.*, 2005, **44**, 3402–3407.
26 Y. Huang, R. Gao, M. Liu, L. Chen, X. Ni, X. Xiao, H. Cong, Q. Zhu, K. Chen and Z. Tao, *Angew. Chem., Int. Ed.*, 2020, DOI: 10.1002/anie.202002666.
27 F. Wu, L. H. Wu, X. Xiao, Y. Q. Zhang, S. F. Xue, Z. Tao and A. I. Day, *J. Org. Chem.*, 2012, **77**, 606–611.
28 L. M. Zheng, J. N. Zhu, Y. Q. Zhang, Q. J. Zhu, S. F. Xue, Z. Tao, J. X. Zhang, Z. Xin, Z. B. Wei, L. S. Long and A. I. Day, *Supramol. Chem.*, 2008, **20**, 709–716.